# Computational Imaging for Correction of non-isoplanatic Aberrations in Optical Wafer Metrology

Wim M.J. Coene, S. Konijnenberg, A. Koolen, T. Tukker, M. van Kraaij, A. den Boef, R.D. Buijs, T.T.M. van Schaijk, T. Cromwijk, M. Adhikary, C. Messinis

November 3, 2022, Paris

MathMet 2022
Session-2
13:20-13:40

# Optical Wafer Metrology and *Holistic Patterning* in Lithography

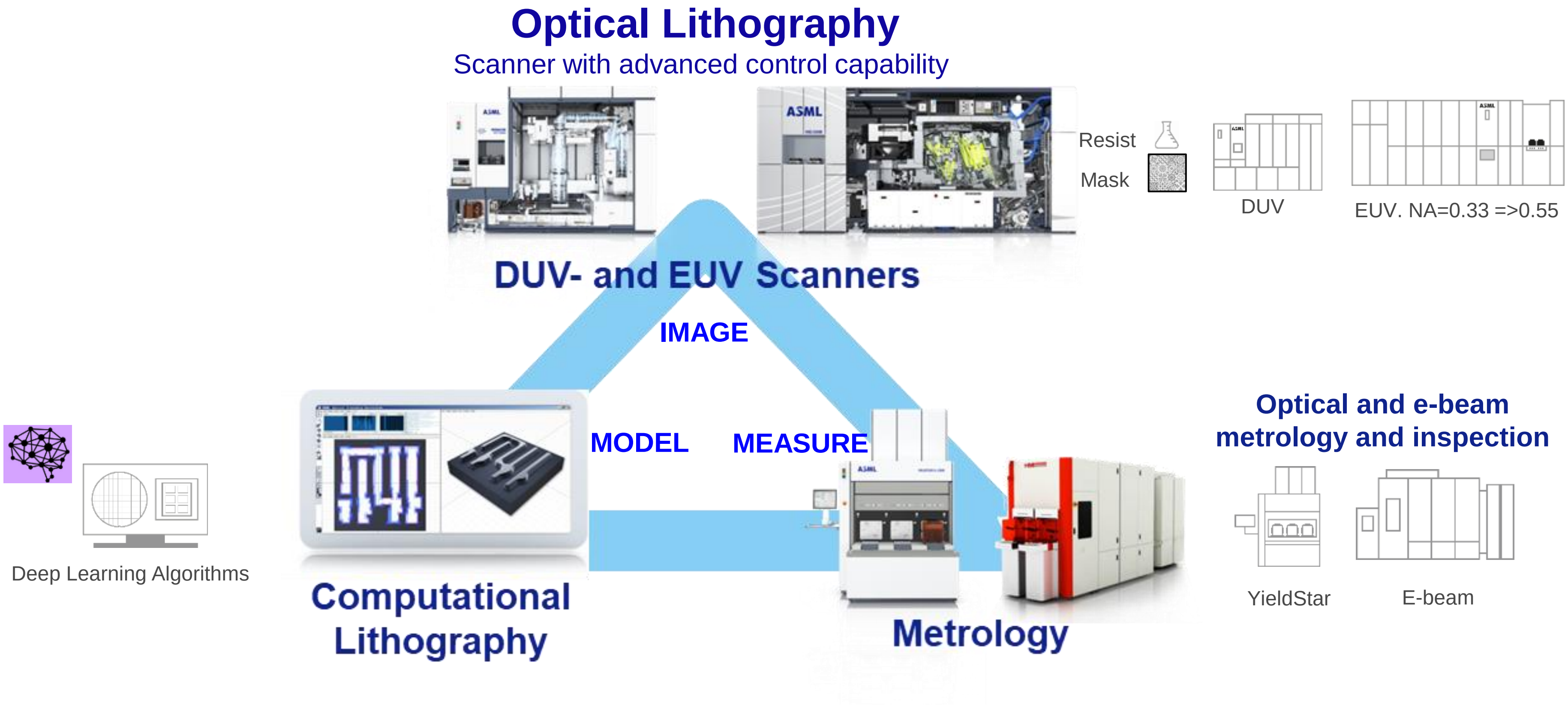



Public

# Optical Metrology : diffraction-based overlay metrology (DBO)

YieldStar


Set of 4 intensities yields overlay

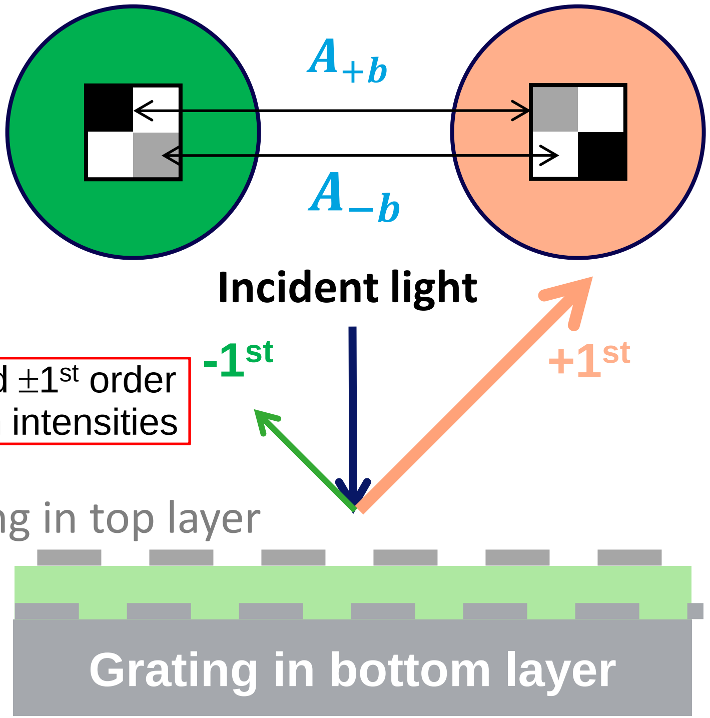


measured ±1st order diffraction intensities

Diffraction Asymmetries

$$I^{+1}_{+b} - I^{-1}_{+b} = A_{+b}$$

$$I^{+1}_{-b} - I^{-1}_{-b} = A_{-b}$$

Dark-Field Image

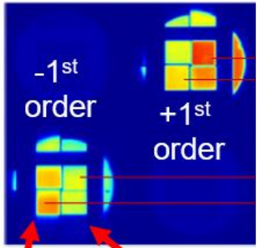


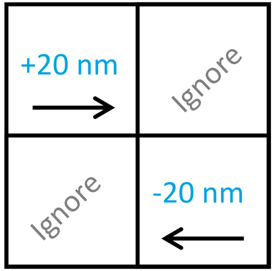


μDBO target on Wafer
10x10 μm²

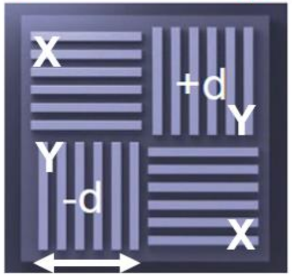


5-8 μm

Target-on-Wafer

| | |
|---|---|
| DBO | diffraction-based overlay (metrology) |
| μDBO | small-target DBO |
| OV | overlay |

ASML

# Some Views on Our Research Landscape (for wafer metrology)

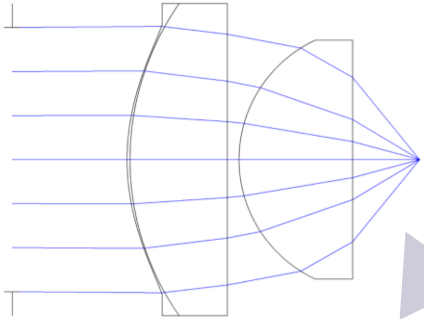

**Optical Wafer Metrology (≥2030)**

**optics design simple optics (low cost)**

**large wavelength range 400-1600nm (applications)**

**4D-aberrations / non-isoplanatism**

**linear imaging system** (fully coherent or incoherent)

***Inverse Problem* of digital 4D-aberration correction**

# 2D-aberrations versus 4D-aberrations
## (isoplanatic versus non-isoplanatic)

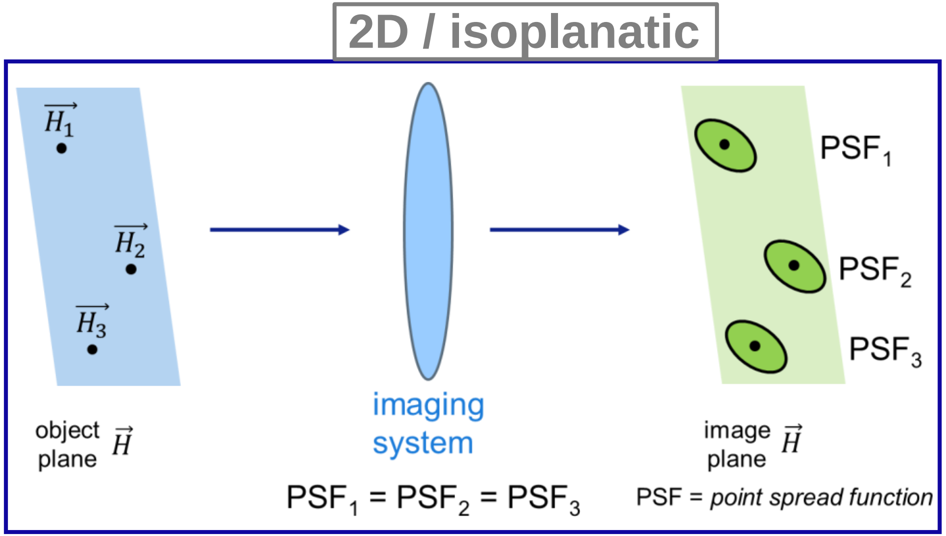


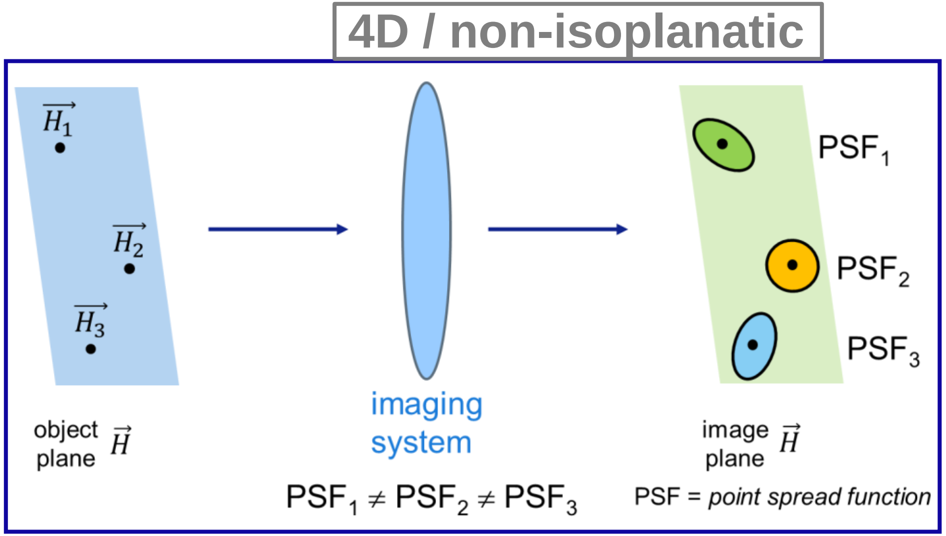


PSF is constant over the field

PSF depends on field-position

# 2D-aberrations versus 4D-aberrations
## (isoplanatic versus non-isoplanatic)

### 2D / isoplanatic

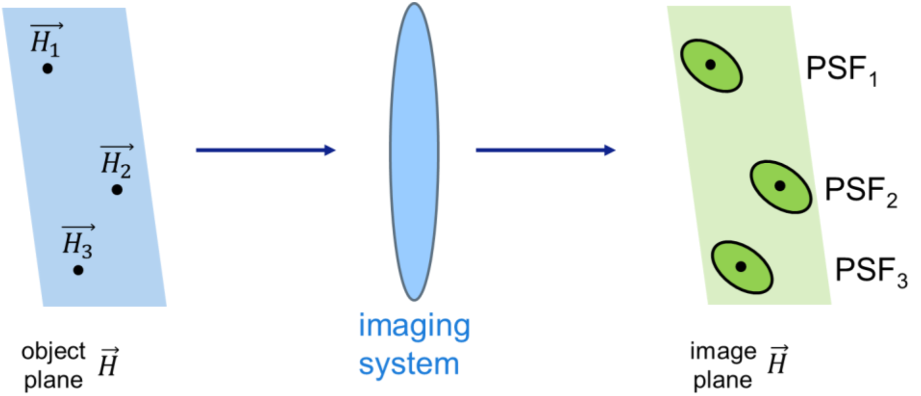


PSF$_1$ = PSF$_2$ = PSF$_3$  PSF = *point spread function*

### Isoplanatic Computational Imaging

$\vec{H}$ (real space)

$$i(\boldsymbol{H}) = h(\boldsymbol{H}) * o(\boldsymbol{H})$$

image wave — 2D PSF — object wave

2D-FT ↓

$\vec{\rho}$ (Fourier space)

$$\tilde{\imath}(\boldsymbol{\rho}) = \tilde{h}(\boldsymbol{\rho}) \cdot \tilde{o}(\boldsymbol{\rho})$$

transfer function

de-convolution ↓

$\vec{\rho}$ (Fourier space)

$$\hat{\tilde{o}}(\boldsymbol{\rho}) = \frac{\tilde{h}^*(\boldsymbol{\rho})}{\left|\tilde{h}(\boldsymbol{\rho})\right|^2 + \varepsilon} \cdot \tilde{\imath}(\boldsymbol{\rho})$$

2D-FT$^{-1}$ ↓

$\vec{H}$ (real space)

$$\hat{o}(\boldsymbol{H})$$

$\boldsymbol{H}$ field space (real space)

$\boldsymbol{\rho}$ pupil space (Fourier space)

$$\underbrace{\tilde{h}(\boldsymbol{\rho})}_{\text{transfer function}} = \underbrace{A(\boldsymbol{\rho})}_{\text{aperture function}}\, e^{i\underbrace{W(\boldsymbol{\rho})}_{\text{wave aberration function}}}$$

Zernike expansion

! NOT POSSIBLE in case of Non-Isoplanatic Imaging !

since $W_{non-isopl} = W(\boldsymbol{\rho}, \boldsymbol{H})$ ↘ Hopkins expansion

# Hopkins' Expansion of 4D wave-aberration function

(rotationally symmetric system)

$\vec{H}$ field (real space)

$\vec{\rho}$ pupil (Fourier space)

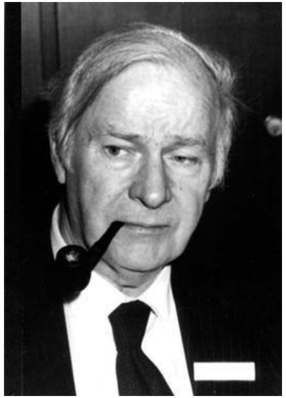

Hopkins (1918-1994)

$$(H^2)^j\left(\vec{H}\cdot\vec{\rho}\right)^m(\rho^2)^n$$

| Aberration name | Vector form | Algebraic form | $j$ | $m$ | $n$ |
|---|---|---|---|---|---|
| *Zero order* | | | | | |
| Uniform piston | $W_{000}$ | $W_{000}$ | 0 | 0 | 0 |
| *Second order* | | | | | |
| Quadratic piston | $W_{200}(\vec{H}\cdot\vec{H})$ | $W_{200}H^2$ | 1 | 0 | 0 |
| Magnification | $W_{111}(\vec{H}\cdot\vec{\rho})$ | $W_{111}H\rho\cos(\phi)$ | 0 | 1 | 0 |
| Focus | $W_{020}(\vec{\rho}\cdot\vec{\rho})$ | $W_{020}\rho^2$ | 0 | 0 | 1 |
| *Fourth order* | | | | | |
| Spherical aberration | $W_{040}(\vec{\rho}\cdot\vec{\rho})^2$ | $W_{040}\rho^4$ | 0 | 0 | 2 |
| Coma *pupil* distortion | $W_{131}(\vec{H}\cdot\vec{\rho})(\vec{\rho}\cdot\vec{\rho})$ | $W_{131}H\rho^3\cos(\phi)$ | 0 | 1 | 1 |
| Astigmatism | $W_{222}(\vec{H}\cdot\vec{\rho})^2$ | $W_{222}H^2\rho^2\cos^2(\phi)$ | 0 | 2 | 0 |
| Field curvature | $W_{220}(\vec{H}\cdot\vec{H})(\vec{\rho}\cdot\vec{\rho})$ | $W_{220}H^2\rho^2$ | 1 | 0 | 1 |
| Distortion *field* distortion | $W_{311}(\vec{H}\cdot\vec{H})(\vec{H}\cdot\vec{\rho})$ | $W_{311}H^3\rho\cos(\phi)$ | 1 | 1 | 0 |
| Quartic piston | $W_{400}(\vec{H}\cdot\vec{H})^2$ | $W_{400}H^4$ | 2 | 0 | 0 |
| *Sixth order* | | | | | |
| Oblique spherical aberration | $W_{240}(\vec{H}\cdot\vec{H})(\vec{\rho}\cdot\vec{\rho})^2$ | $W_{240}H^2\rho^4$ | 1 | 0 | 2 |
| Coma | $W_{331}(\vec{H}\cdot\vec{H})(\vec{H}\cdot\vec{\rho})(\vec{\rho}\cdot\vec{\rho})$ | $W_{331}H^3\rho^3\cos(\phi)$ | 1 | 1 | 1 |
| Astigmatism | $W_{422}(\vec{H}\cdot\vec{H})(\vec{H}\cdot\vec{\rho})^2$ | $W_{422}H^4\rho^2\cos^2(\phi)$ | 1 | 2 | 0 |
| Field curvature | $W_{420}(\vec{H}\cdot\vec{H})^2(\vec{\rho}\cdot\vec{\rho})$ | $W_{420}H^4\rho^2$ | 2 | 0 | 1 |
| Distortion | $W_{511}(\vec{H}\cdot\vec{H})^2(\vec{H}\cdot\vec{\rho})$ | $W_{511}H^5\rho\cos(\phi)$ | 2 | 1 | 0 |
| Piston | $W_{600}(\vec{H}\cdot\vec{H})^3$ | $W_{600}H^6$ | 3 | 0 | 0 |
| Spherical aberration | $W_{060}(\vec{\rho}\cdot\vec{\rho})^3$ | $W_{060}\rho^6$ | 0 | 0 | 3 |
| Un-named | $W_{151}(\vec{H}\cdot\vec{\rho})(\vec{\rho}\cdot\vec{\rho})^2$ | $W_{151}H\rho^5\cos(\phi)$ | 0 | 1 | 2 |
| Un-named | $W_{242}(\vec{H}\cdot\vec{\rho})^2(\vec{\rho}\cdot\vec{\rho})$ | $W_{242}H^2\rho^4\cos^2(\phi)$ | 0 | 2 | 1 |
| Un-named | $W_{333}(\vec{H}\cdot\vec{\rho})^3$ | $W_{333}H^3\rho^3\cos^3(\phi)$ | 0 | 3 | 0 |

(Hopkins coefficients; J. Sasian Table 5.1)

# Non-isoplanatic 4D-PSF Forward Model

$$i\left(\vec{H}\right) = \int H_{4D}\left(\vec{H};\vec{H'}\right)\, o\left(\vec{H'}\right) d\vec{H'}$$

image wave 4D-PSF object wave

**matrix notation** $i = H_{4D} \cdot o$

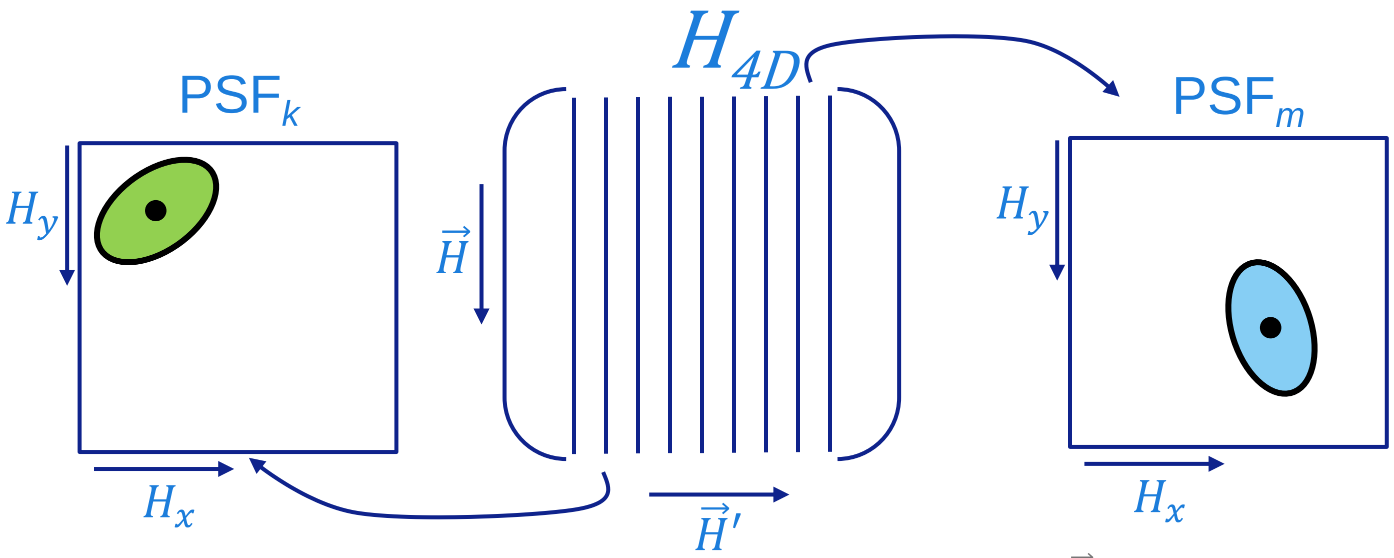


*$H_{4D}$ contains spatially varying* PSFs, dependent on the position $\vec{H}'$ of the point in the object.

# Concept of *Point-per-Point*-Deconvolution for solution of Inverse Problem

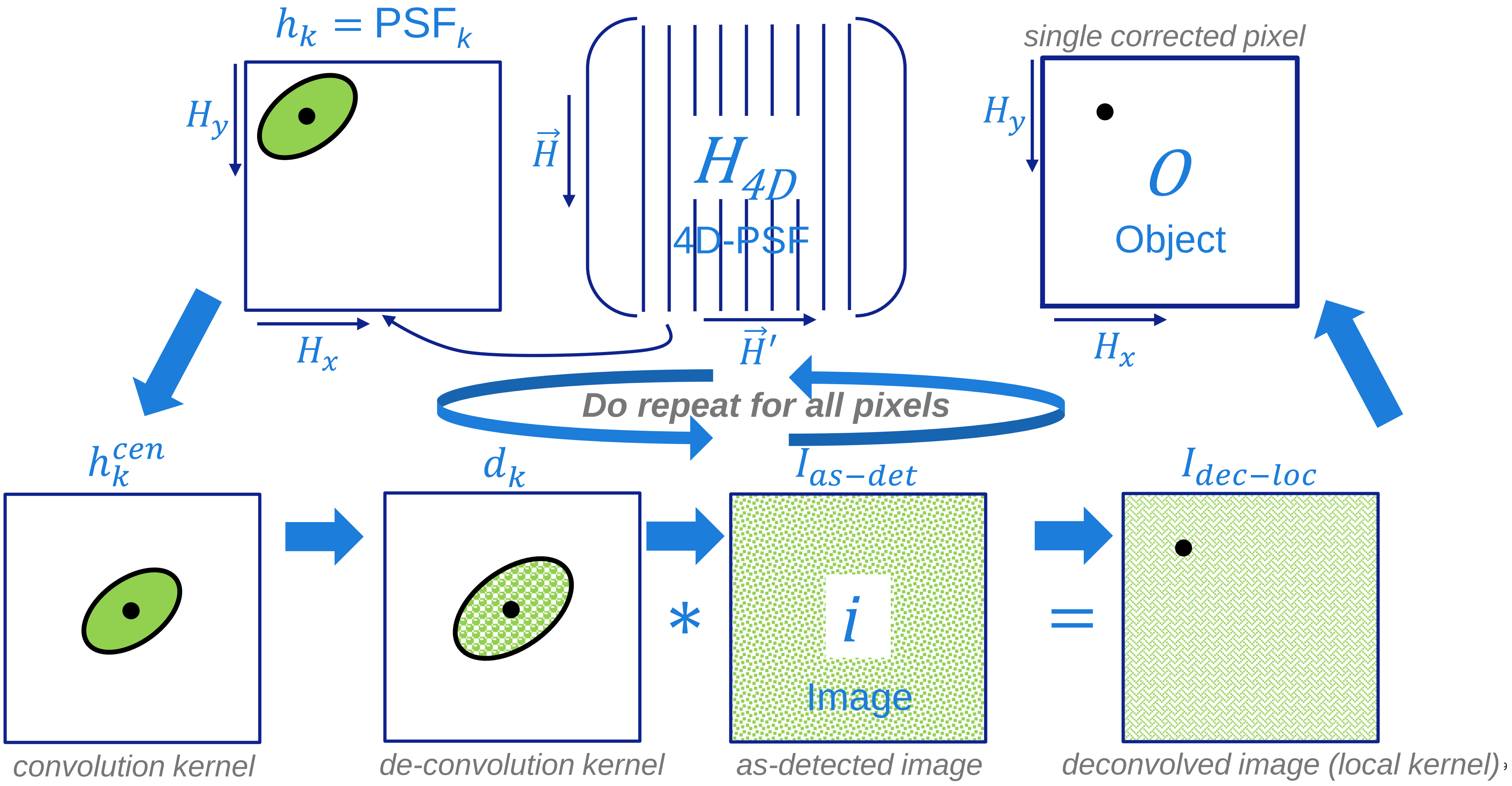

# New Approach: SVD-on-Deconvolution-Kernels for Inverse Problem

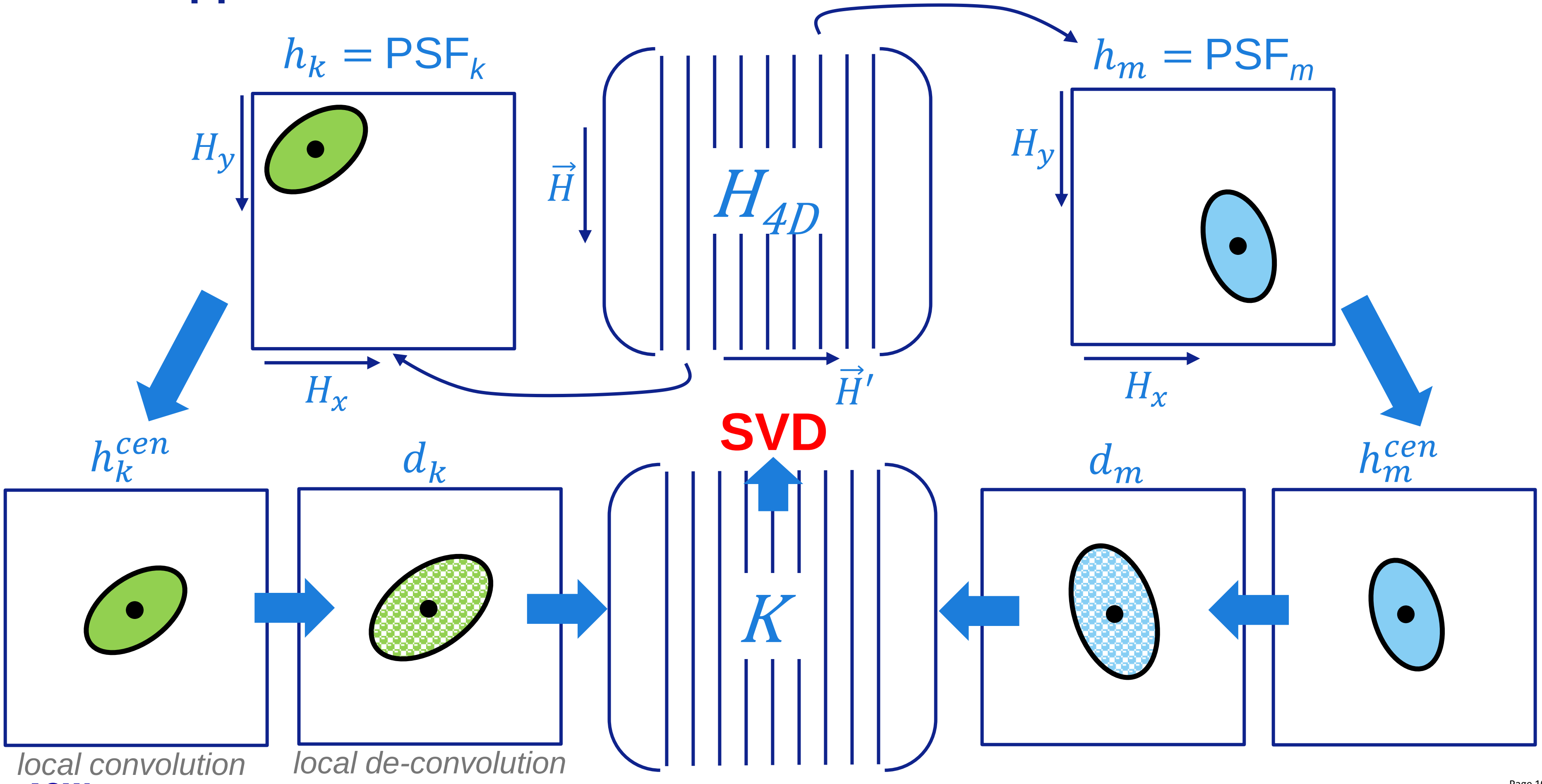


SVD singular value decomposition

# New Approach: SVD-on-Deconvolution-Kernels for Inverse Problem

local
deconvolution-kernels

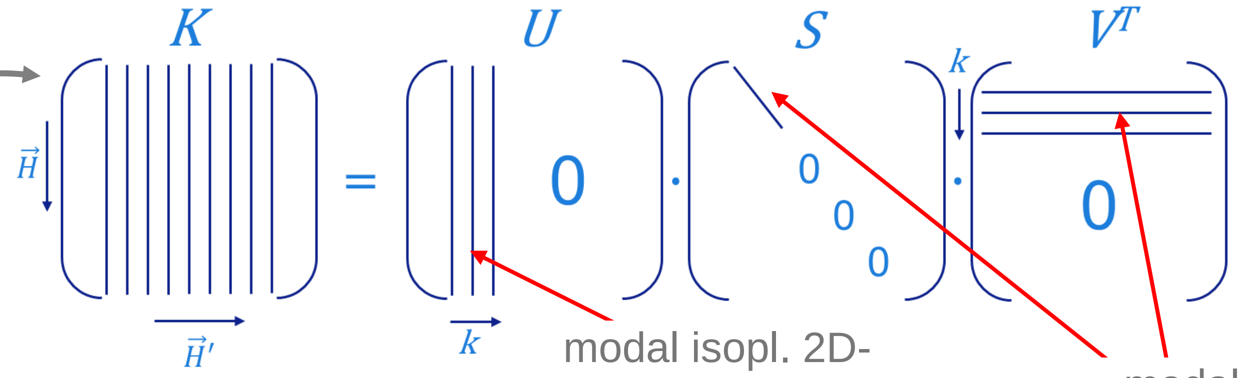


modal isopl. 2D-
deconvolution kernels

modal
2D-weights

*product-convolution*
*series approximation*
of 4D-Deconvolution Kernels

$$D_{4D}\left(\vec{H};\vec{H'}\right) \approx \sum_{k=1}^{k_{max}} \overbrace{p_k\left(\vec{H}-\vec{H'}\right)} \overbrace{w_k\left(\vec{H'}\right)}$$

*SVD-based*
deconvolution
for 4D-aberrations
(~ $k_{max}$ FFTs)

$$\boxed{\underset{\text{object-field}}{\hat{o}\left(\vec{H}\right)} \approx \sum_{k=1}^{k_{max}} p_k\left(\vec{H}\right) * \left[w_k\left(\vec{H}\right) \underset{\text{image-field}}{i\left(\vec{H}\right)}\right]}$$

***$k_{max}$** isoplanatic modal deconvolutions on spatially weighted versions of the measured image field i.*

# Two Strategies for 4D Aberration Correction

| **Strategy-1**<br>**1-step Approach** | **Strategy-2**<br>**3-step Approach** |
|---|---|
| 1. **SVD-based Deconvolution** for all 2D & 4D aberrations in one go. | 1. **Isoplanatic Deconvolution** with the deconvolution kernel for the PSF at one chosen location. |
| - | 2. **Pupil Distortion Correction** (by *remapping* of pupil (Fourier) space due to W131, W151, …) |
| - | 3. **SVD-based Deconvolution** for all remaining 4D aberrations. |
| **PRO**<br>One single framework | **PRO**<br>Computational efficiency |

# Dark-Field Holographic Microscope (DHM)

Experimental
DHM set-up
@ VU-ARCNL

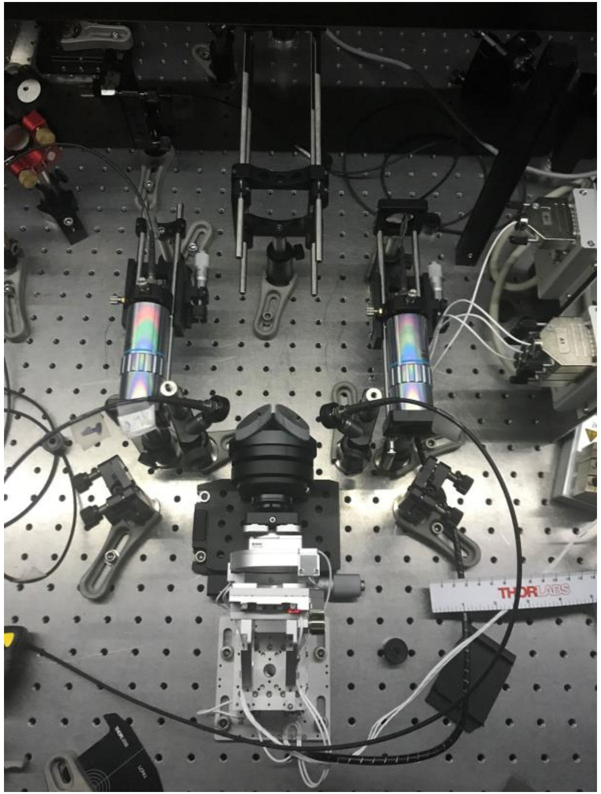


$\lambda$ = 532nm / 632nm

NA = 0.80

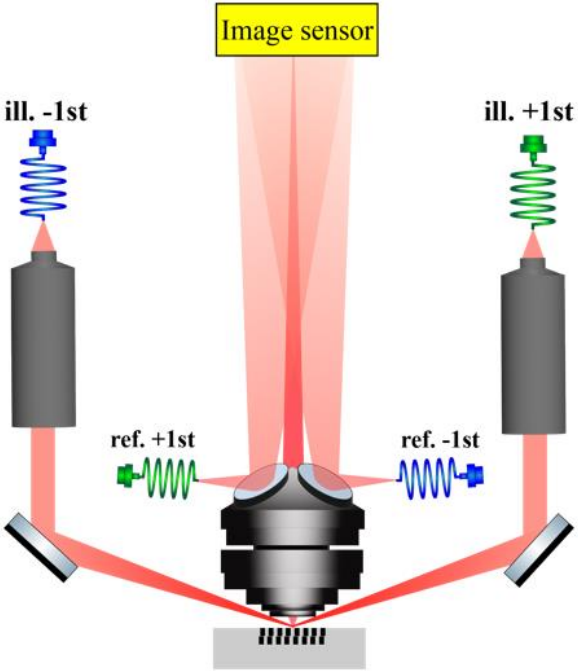


Schematics of
DHM set-up
@ VU-ARCNL

- off-axis holography
- measurement of amplitude and phase
  of the image field from the *sideband* of the hologram

# 4D-PSF Calibration via 2D-array of Nanoholes

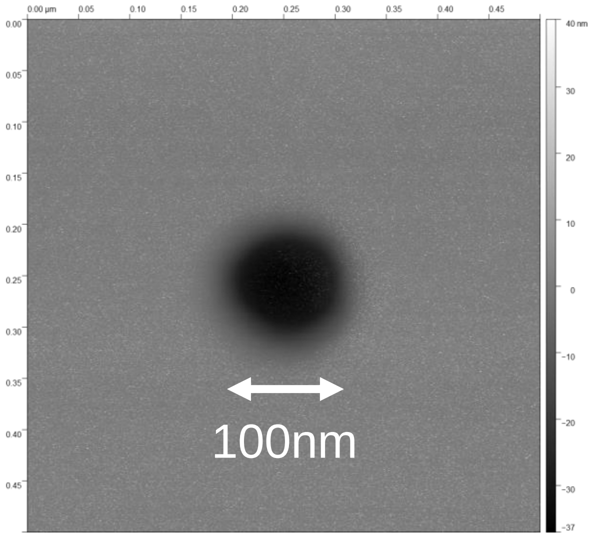


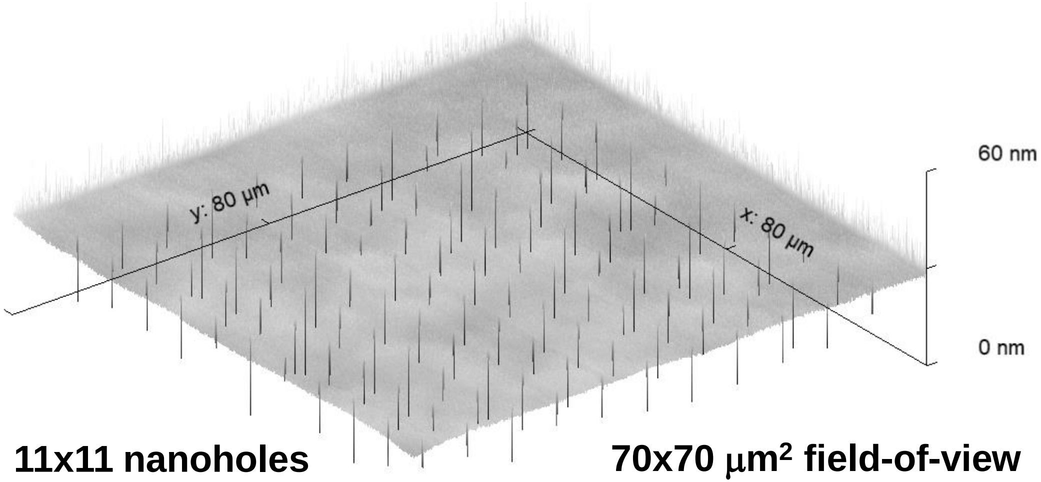


**11x11 nanoholes** **70x70 $\mu m^2$ field-of-view**

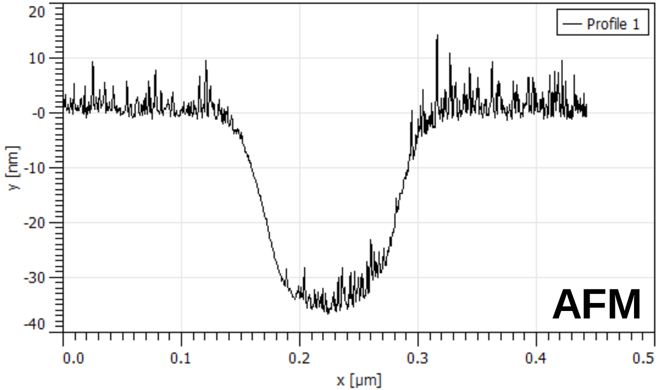


- Nanoholes acts as $\delta$-functions

- Nanoholes probe the spatial variation of the 4D-PSFs as measured directly via the sideband of the hologram.

# 4D-PSF Calibration via 2D-array of Nanoholes

Measured PSFs

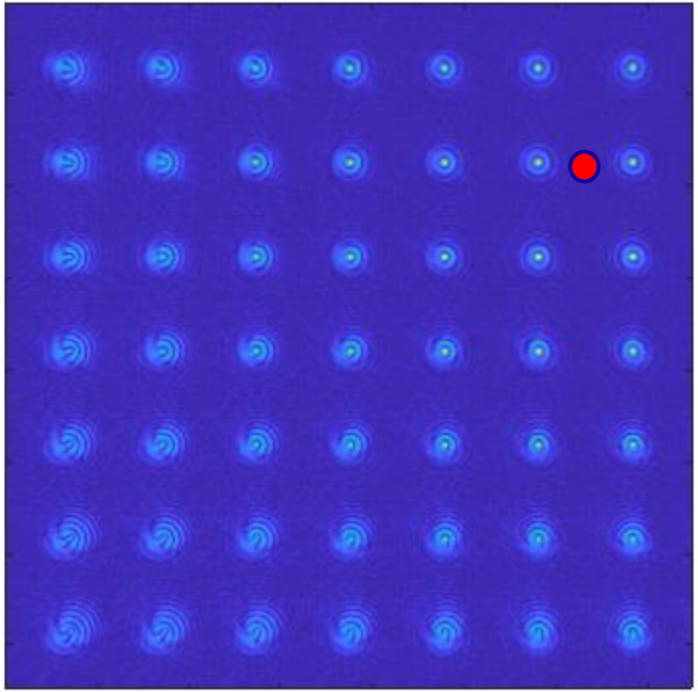

**Simulated PSFs (from parameters Optics Design)**

abs all 11x11 PSFs at 532nm at 7um distance

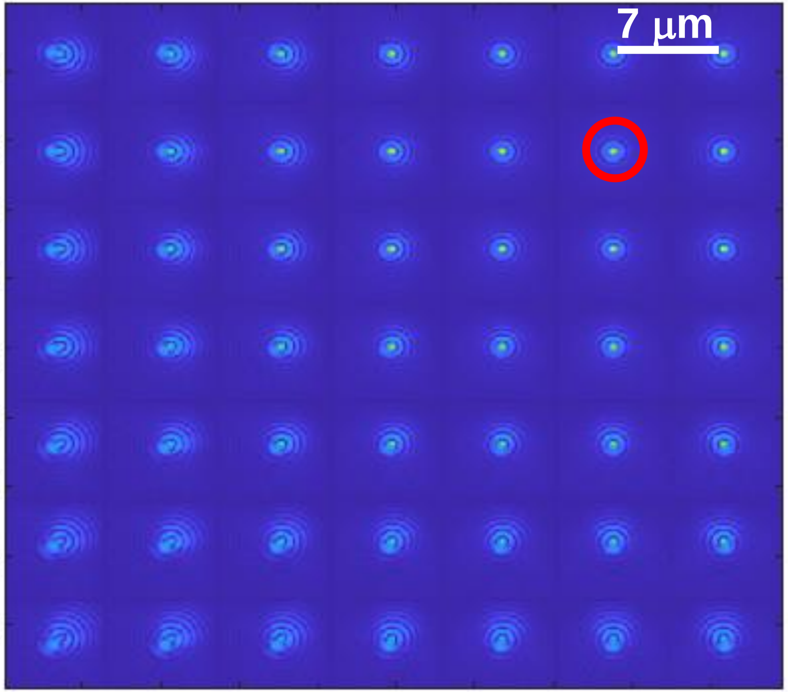


$\lambda$ = 532nm

NA = 0.80

7x7 SW-subset of 11x11 nanohole array

assumed position
of *nodal point*
(= origin of field space)

ASML



Public

# 4D-PSF Calibration via 2D-array of Nanoholes

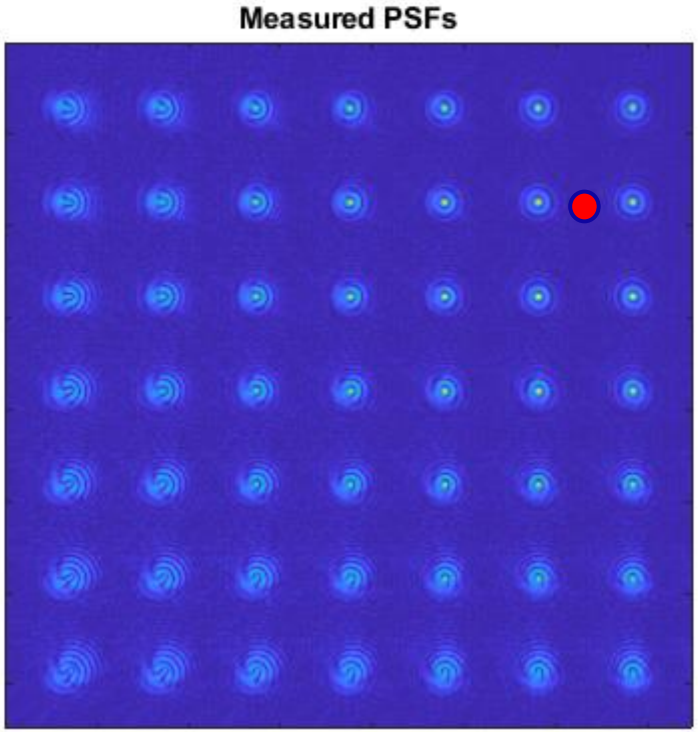


assumed position
of *nodal point*
(= origin of field space)

$\lambda$ = 532nm

NA = 0.80

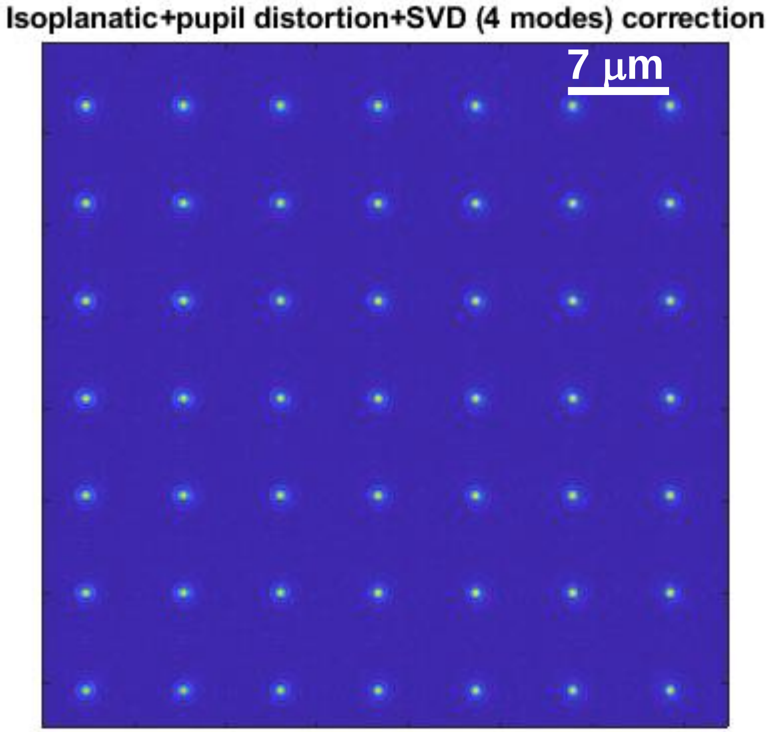


7x7 SW-subset of 11x11 nanohole array



Public

# 4D-PSF Calibration via 2D-array of Nanoholes

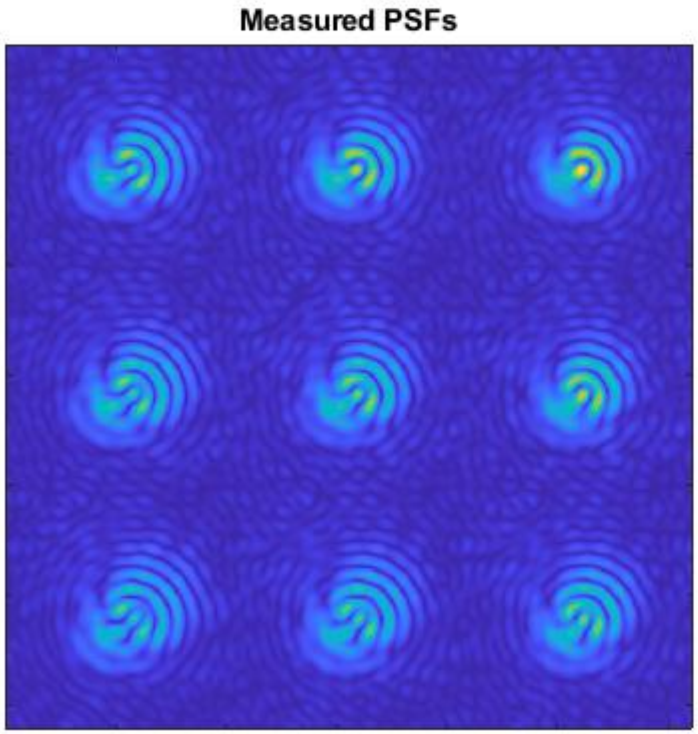


$\lambda$ = 532nm

NA = 0.80

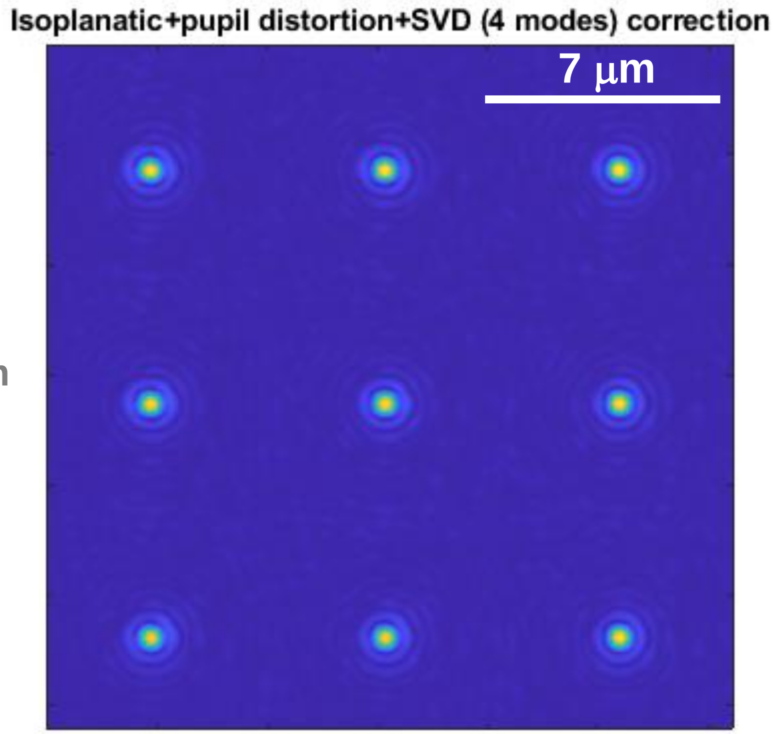

# 4D Aberration Correction for Array of Grating Pads

**No Correction, *as-detected.***

λ = 632nm

NA = 0.80

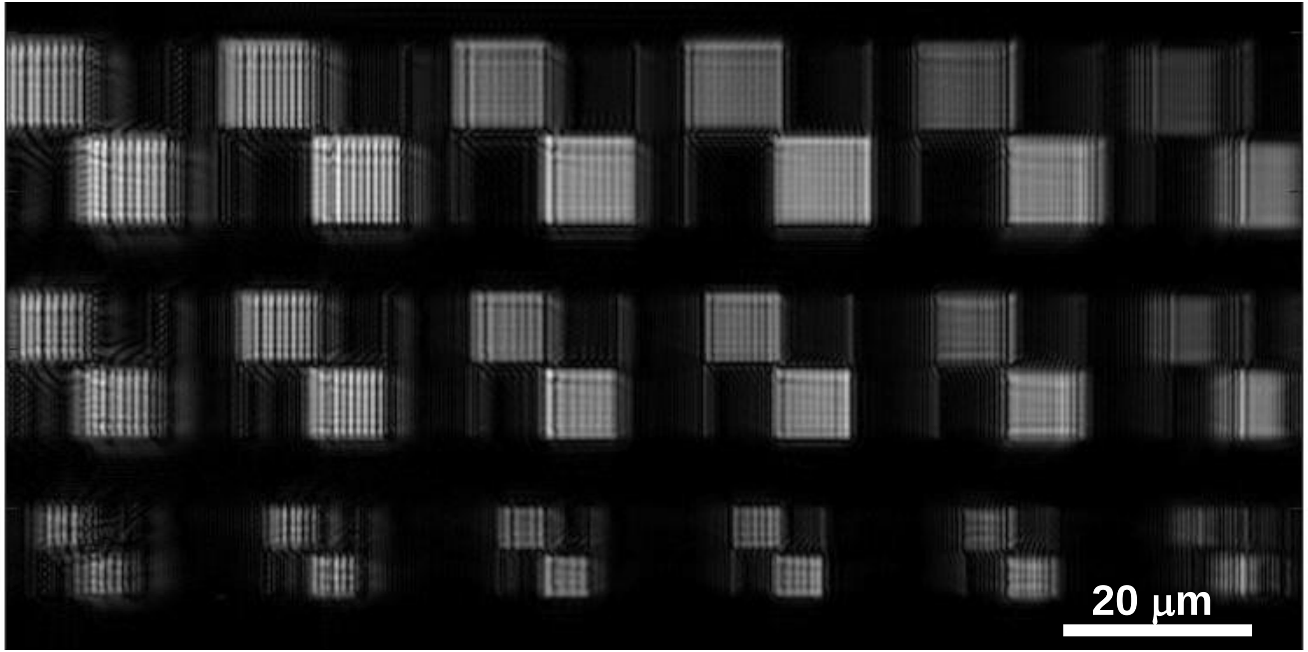


C20

C15

C10

pitches: 900nm 800nm 700nm 600nm 500nm 400nm

# 4D Aberration Correction for Array of Grating Pads

**Full Correction, isopl. + pupil disto.corr. + SVD + *digital focus.***

$\lambda$ = 632nm

NA = 0.80

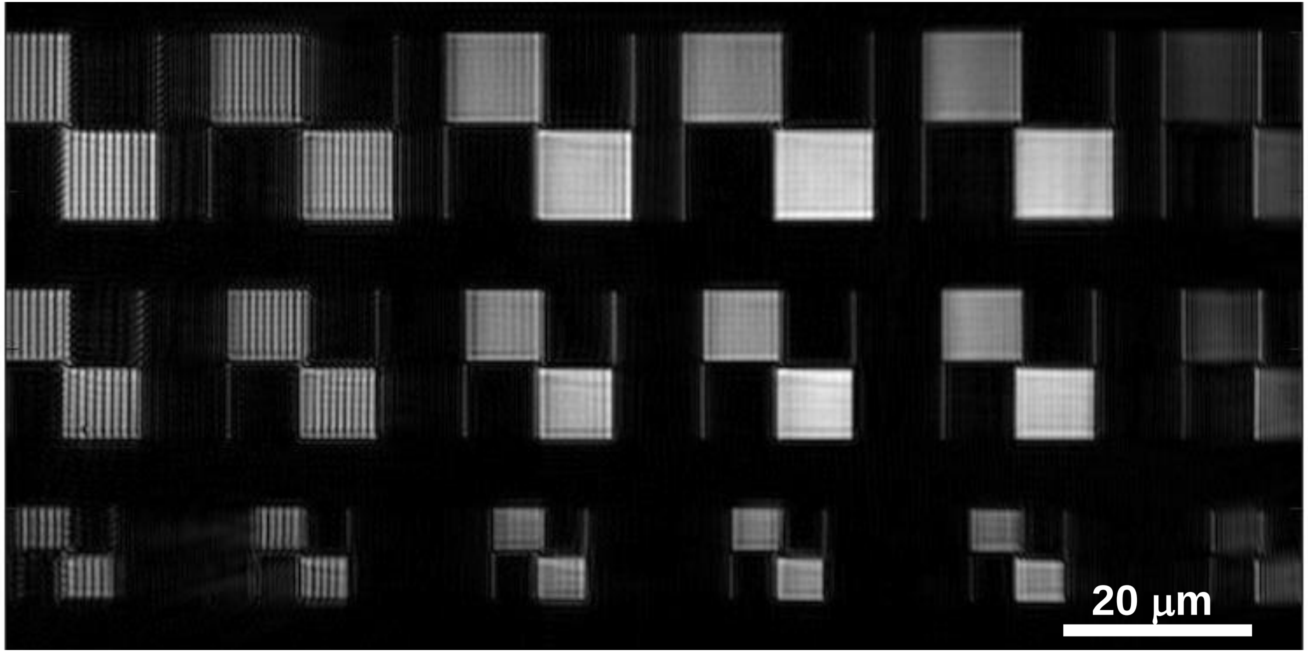


C20

C15

C10

pitches: 900nm 800nm 700nm 600nm 500nm 400nm


Public

# 4D Aberration Correction for Array of Grating Pads

**Full Correction, isopl. + pupil disto.corr. + SVD + *NO digital focus.***

λ = 632nm

NA = 0.80

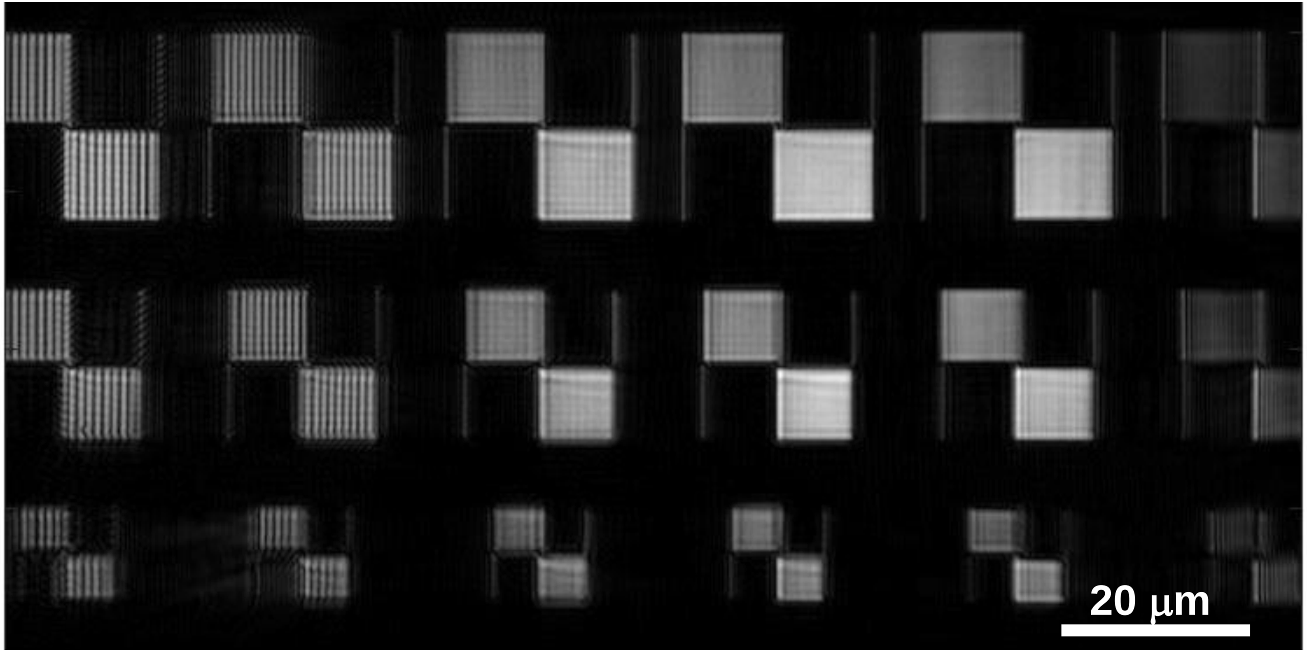


C20

C15

C10

pitches: 900nm 800nm 700nm 600nm 500nm 400nm

# Some Extra Thoughts

- Non-isoplanatism can be caused by at least 3 effects:

  - 4D aberrations of the imaging optics
  - *Surface roughness* of the multiple lens components
  - *Field-position dependent apodization* in Holographic Microscopy, see submitted paper to Optics Express (Sept. 2022):

**Field-position dependent apodization in dark-field Digital Holographic Microscopy for semiconductor metrology**

TAMAR CROMWIJK,[1,2,*] MANASHEE ADHIKARY,[1,2] CHRISTOS MESSINIS,[3] SANDER KONIJNENBERG,[3] WIM COENE,[3] STEFAN WITTE,[1,2] JOHANNES F. DE BOER,[1] AND ARIE DEN BOEF[1,2,3]

- Other areas of Application:

  - Correction for Spatially Varying Blur in **Incoherent Imaging** in Astronomy
    - See: L. Denis, E. Thiebaut, F. Soulez, J.-M. Becker, R. Mourya, *Fast Approximations of Shift-Variant Blur*, Int. J. Comput. Vis. Vol. 115, 2015, pp. 253-278
    - Based on MSE-optimization using an **iterative approach**

# Conclusions

- Deconvolution for 4D field-dependent non-isoplanatic aberrations is feasible for coherent imaging in off-axis holography at low computational costs.

- A computationally efficient SVD-based deconvolution strategy has been proposed.

- The SVD-based deconvolution can be combined with two prior steps of

  (a) isoplanatic deconvolution
  (b) pupil distortion correction

  in order to further increase computational efficiency.

- Very first experimental data as acquired with Dark-Field Holographic Microscopy have shown a first proof of concept of our 4D aberration correction strategy.

# Thank you!

Wim Coene
ASML Research
CMMS-group

wim.coene@asml.com

Veldhoven